Neuroscience Letters 480 (2010) 148–153

Contents lists available at ScienceDirect

Neuroscience Letters

journal homepage: www.elsevier.com/locate/neulet

# Spectral receptive field properties of visually active neurons in the caudate nucleus

Attila Nagy[a,*], Antal Berényi[a], Marek Wypych[b], Wioletta J. Waleszczyk[b], György Benedek[a]

[a] Department of Physiology, Faculty of Medicine, University of Szeged, Dóm tér 10, H-6720 Szeged, Hungary
[b] Department of Neurophysiology, Nencki Institute of Experimental Biology, 3 Pasteur St., 02-093 Warsaw, Poland

ARTICLE INFO

*Article history:*
Received 2 April 2010
Received in revised form 4 June 2010
Accepted 9 June 2010

*Keywords:*
Visual receptive fields
Striatum
Spatial tuning
Temporal tuning
Speed tuning
Cat

ABSTRACT

Recent studies stress the importance of the caudate nucleus in visual information processing. Although the processing of moving visual signals depends upon the capability of a system to integrate spatial and temporal information, no study has investigated the spectral receptive field organization of the caudate nucleus neurons yet. Therefore, we tested caudate neurons of the feline brain by extracellular single-cell recording applying drifting sinewave gratings of various spatial and temporal frequencies, and reconstructed their spectral receptive fields by plotting their responsiveness as a function of different combinations of spatial and temporal frequencies. The majority of the caudate cells (74%) exhibited peak tuning, which means that their spatio-temporal frequency response profile had a characteristic region of increased activity with a single maximum in the spatio-temporal frequency domain. In one-quarter of the recorded caudate neurons ridge tuning was found, where the region of increased activity, forming an elongated ridge of maximal sensitivity parallel or angled to the spatial or the temporal frequency axis, indicating temporal (16%), spatial (5%) or speed (5%) tuning, respectively. The velocity preference of the ridge tuned caudate nucleus neurons is significantly lower than that of the peak tuned neurons. The peak tuned neuron could encode high velocities, while the ridge tuned neurons were responsible for the detection of moderate and lower velocities. Based upon our results, we suggest that the wide variety of spatio-temporal frequency response profiles might represent different functional neuronal groups within the caudate nucleus that subserve different behaviors to meet various environmental requirements.


Previous studies demonstrated that the CN plays a prominent role by processing multisensory information, thus orchestrating the sensorimotor and visuomotor coordination [1,6,9]. Accordingly, a number of studies were performed to clarify the exact role of the CN in visual information processing [2,6,11,17,18,20,21]; the results of these experiments can be summarized as follows: anatomical studies suggest that there are two sets of neural circuits that are involved in the transmission of visual information from the retina to the CN. First, visual information might reach this structure through a descending cortico-striatal route [5,7,14,19]. Second, the CN neurons might receive their visual input through the ascending tectofugal system [8]. The visual receptive field properties of the CN neurons and their sensitivity to visual stimuli of low spatial and high temporal frequency makes them very similar to the neurons of the superior colliculus (SC) and those of the other structures of the ascending tectofugal system [10,12,15,16]. It is noteworthy that these stimulus preferences are in sharp contrast with the properties of the neurons of the geniculostriate pathway, supporting the notion that the particular dynamic properties of visual information processing in the CN is different from those observed in the lateral geniculate nucleus of the thalamus and in the primary visual cortex. Although the processing of moving visual signals depends critically upon the ability of a system to integrate spatial and temporal information [4,16], no study has described spectral receptive field organization of the CN neurons yet. In the present study, therefore, we tested the CN neurons of the feline brain by applying a wide range of drifting sinewave gratings of various spatial and temporal frequencies and reconstructed their spectral receptive fields. These 3D graphs were generated by plotting their responsiveness as a function of the different spatial and temporal frequency combinations [23]. Our main goal was to characterize different functional neuronal groups within the CN according to their spatio-temporal spectral receptive field organization. Moreover, we compared the spectral receptive field organization of CN neurons to that of the SC neurons [23], in order to test our current hypothesis about a functional connection between the CN and the ascending tectofugal system.

Five adult cats of either sex weighing from 2.4 to 3.5 kg were used in this study. All experimental procedures were carried out

* Corresponding author at: Department of Physiology, University of Szeged, Dóm tér 10, H-6720 Szeged, POB 427, Hungary. Tel.: +36 62 545869; fax: +36 62 545842.
*E-mail address:* nagya@phys.szote.u-szeged.hu (A. Nagy).

0304-3940/$ – see front matter © 2010 Elsevier Ireland Ltd. All rights reserved.
doi:10.1016/j.neulet.2010.06.030

to minimize the number of the animals and followed the European Communities Council Directive of 24 November 1986 (S6 609 EEC) and National Institutes of Health guidelines for the care and use of animals for experimental procedures. The experimental protocol had been approved by the Ethical Committee for Animal Research of Albert Szent-Györgyi Medical and Pharmaceutical Center of the University of Szeged. The animals were initially anaesthetized with ketamine hydrochloride (30 mg/kg i.m., Calypsol). To reduce salivation and bronchial secretion a subcutaneous injection of 0.2 ml 0.1% atropine sulphate was administered preoperatively. The trachea and the femoral vein were cannulated and the animals were placed in a stereotaxic headholder. All wounds and pressure points were routinely infiltrated with local anesthetic (procaine hydrochloride, 1%). Throughout the surgery the anesthesia was maintained with halothane (1.6%, fluothane) in air. The animals were immobilized with gallamine triethiodide (20 mg/kg). During recording sessions gallamine triethiodide (8 mg/kg/h), glucose (10 mg/kg/h) and dextran (50 mg/kg/h) in Ringer lactate solution was infused at a rate of 4 ml/h. Atropine sulphate (1–2 drops, 0.1%) and phenylephrine hydrochloride (1–2 drops, 10%) were applied locally to dilate the pupils, block accommodation, and retract the nictitating membranes. The eye contralateral to the recording side was supported with a +2 dioptre contact lens. The ipsilateral eye was occluded during the visual stimulation. During the recording sessions, anesthesia was maintained with a gaseous mixture of air and halothane (about 0.8%). The end-tidal concentration of halothane, MAC values and peak $CO_2$ concentrations were monitored with a capnometer (Capnomac Ultima, Datex-Ohmeda, Inc.). The heart rate and brain activity (ECG and EEG) were also monitored continuously. During the length of the anesthesia the EEG indicated slow wave sleep. The peak expired $CO_2$ was kept in the range of 3.8–4.2%. The body temperature was maintained at approx. 37 °C using a warm-water heating blanket with thermostat.

Electrophysiological recordings of single units were carried out extracellularly via tungsten microelectrodes (AM System, Inc., USA; 2–4 MΩ). Vertical penetrations were made between the Horsley–Clarke co-ordinates anterior: 12–16, lateral: 4–6.5 in the stereotaxic depths 12–19, to record the activity of CN neurons. Single-cell discrimination was performed with a spike-separator system (SPS-8701, Australia), after high-pass filtering the recorded signal (>500 Hz). At the end of the experiments, the animals were deeply anesthetized with pentobarbital (200 mg/kg i.v.) and perfused transcardially with 4% paraformaldehyde solution. The brains were removed and cut into coronal sections of 50 μm, and the sections were stained with Neutral Red. Recording sites were localized on the basis of the marks of the electrode penetrations. The recorded neurons were located in the dorsolateral aspect of the CN.

Spatio-temporal frequency characteristics of each unit were tested with drifting sinewave gratings displayed on a CRT monitor (refresh rate: 85 Hz) positioned at a distance of 42.5 cm away from the cat's eye. To obtain the most preferred direction of movement for each cell, gratings were moved in eight different directions (0–315° at 45° increments). The preferred direction was then used for determination of the spatio-temporal frequency characteristics of the tested cell. The contrast of the grating was held constant at 96% (Michelson contrast = $(L_{max} - L_{min})/(L_{max} + L_{min})$, where $L_{max}$ and $L_{min}$ are the maximum and minimum luminance of the spatial sinusoid, respectively). The mean luminance of the screen was 23 cd/m$^2$. Stimuli were presented on the monitor masked by a circular aperture with a diameter of 30°, centred on the area centralis. The spatio-temporal frequency response profiles of CN cells were assessed using 24–93 spatio-temporal frequency combinations of drifting gratings. The tested spatial frequencies ranged from 0.025 to 0.54 cycles/° (c/°), while the temporal frequencies varied from 0.07 to 29.24 cycles/s (Hz). Responses to stimulus movement were averaged over all presentations of the given spatio-temporal frequency combination. Each spatio-temporal frequency combination was presented at least 12 times. The presentation of the single stimulus overall lasted 2 s. During the first 1 s, the grating remained stationary, and was then drifted for another 1 s. The interstimulus interval was 0.5 s, while blank screen was shown. Peristimulus time histograms (PSTHs) were constructed online to visualize neuronal activity. The net discharge rate, calculated as the difference between the mean firing rates of the cell obtained during stimulus movement and the 400 ms long period (prestimulus period; the first 600 ms of the neuronal responses to stationary stimulus was truncated, to void the response given to the luminance change due to the onset of stationary grating) preceding the onset of movement, was used to characterize the response amplitude of the CN neurons. Cells with non-stimulus related changes in neuronal activity during recording, i.e. when the mean 'spontaneous' (background) activity of the cell varied more than 2 SEM of the mean 'spontaneous' were excluded from the analysis.

The spatio-temporal receptive fields (spectral RFs) were constructed by fitting a surface to the three-dimensional matrices of response strength (e.g. Fig. 1) (MATLAB® software, MathWorks, Inc.). For most of the cells, the response to spatial frequency depended on the temporal frequency of the drifting grating. The two-dimensional spatio-temporal frequency response profiles of the cell; i.e. transections of the 3D spectral RF maps were presented by fitting the curve to data-points located in the region of peak sensitivity, using triangle-based cubic interpolation (MATLAB®). Here we used principal component analysis (PCA) to find the orientation of the area of response in the two-dimensional spatio-temporal frequency response profile of the cell. PCA was applied (in MATLAB®) to the set of points in which interpolated cell responses exceeded a given threshold (0.5 of the maximum response). The orientation of the transection plane corresponded to the main direction found by PCA. The orientation of the main direction found by PCA can be used to determine the spatio-temporal spectral tuning types of the CN neurons. The region of increased activity and the orientation of the main direction can be parallel or angled to the temporal or the spatial frequency axis, indicating spatial, temporal or speed tuning, respectively (for classification see Ref. [3]).

Statistical results are presented as mean ± standard deviation (SD).

We recorded altogether 111 visually active neurons from the CN. Twenty-eight of the recorded units were excluded from the analysis, as a result of an unstable spontaneous activity. The mean spontaneous activity of the CN neurons was 7.8 ± 5.4 spike/s ($N$ = 83; range: 0–32 spikes/s). In general, the neurons in the CN responded optimally to very low spatial (<0.2 c/°) and moderate and high temporal frequencies (>4 Hz), exhibited low spatial and temporal resolution and narrow spatial and temporal frequency tuning. The majority of the neurons showed low-pass spatial frequency tuning with no or only a slight attenuation of the response at low spatial frequencies. Spatial band-pass units were also recorded but we have not encountered spatial high-pass units. Furthermore, the majority of the neurons showed band-pass temporal frequency tuning with optima in the high temporal frequency range. Temporal high-pass neurons were also found, but we recorded no temporal low-pass units in the CN (for a more detailed description of the spatio-temporal properties of the CN, see our previous publication [13]).

The spatio-temporal frequency response profiles were obtained for 83 CN cells for responses given to the sinusoidal gratings drifting in the optimal direction. The majority of the CN cells exhibited peak tuning (62/83, 74%, Fig. 1), which means that their spatio-temporal frequency response profile had a characteristic region of increased activity with a single maximum in the spatio-temporal frequency domain. The profiles of these spectral RFs indicate the existence of single oval regions of increased activity (Fig. 1C). A

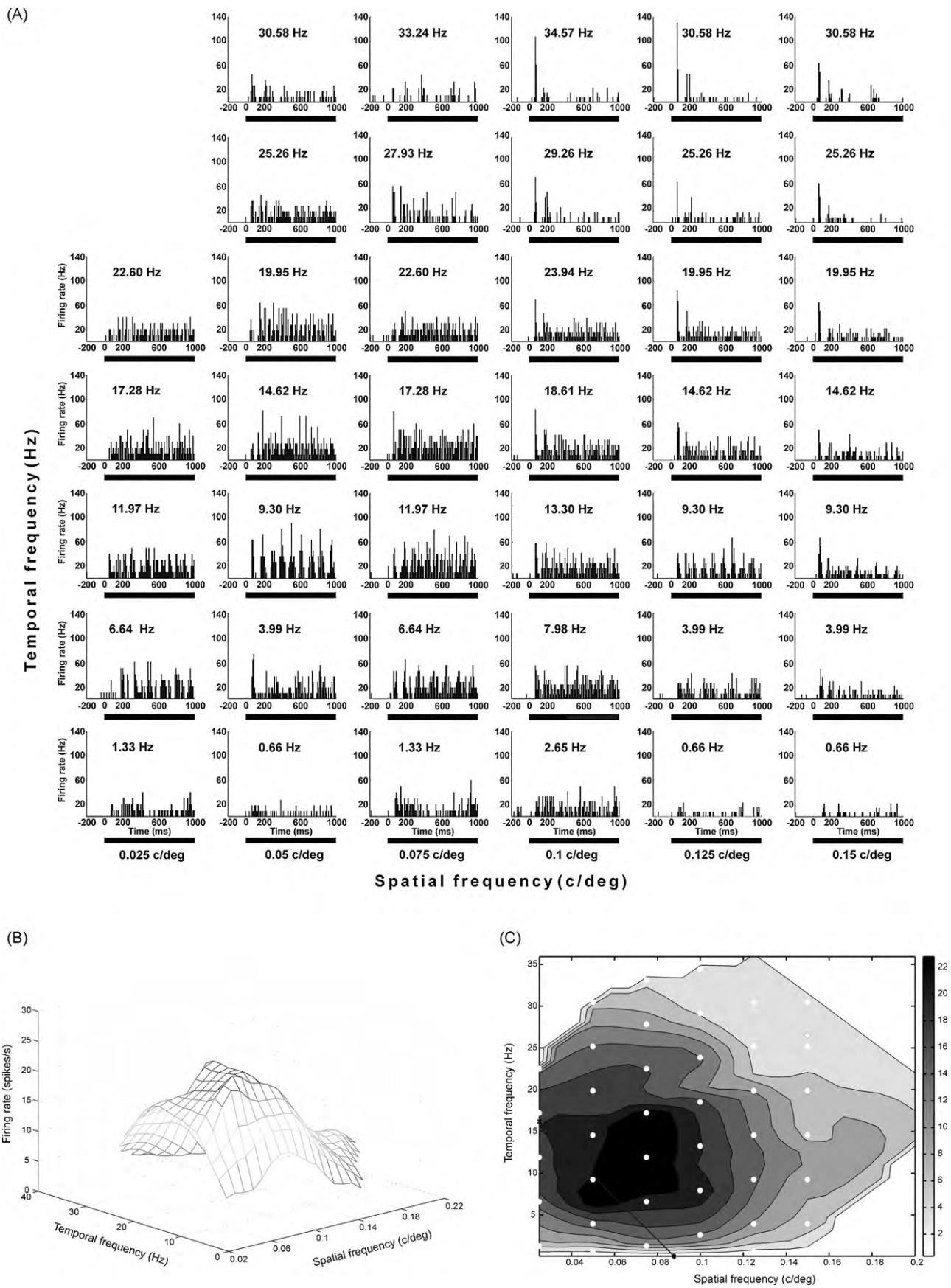
(A)
Temporal frequency (Hz)
Spatial frequency (c/deg)
Firing rate (Hz)
Time (ms)
30.58 Hz
33.24 Hz
34.57 Hz
30.58 Hz
30.58 Hz
25.26 Hz
27.93 Hz
29.26 Hz
25.26 Hz
25.26 Hz
22.60 Hz
19.95 Hz
22.60 Hz
23.94 Hz
19.95 Hz
19.95 Hz
17.28 Hz
14.62 Hz
17.28 Hz
18.61 Hz
14.62 Hz
14.62 Hz
11.97 Hz
9.30 Hz
11.97 Hz
13.30 Hz
9.30 Hz
9.30 Hz
6.64 Hz
3.99 Hz
6.64 Hz
7.98 Hz
3.99 Hz
3.99 Hz
1.33 Hz
0.66 Hz
1.33 Hz
2.65 Hz
0.66 Hz
0.66 Hz
0.025 c/deg
0.05 c/deg
0.075 c/deg
0.1 c/deg
0.125 c/deg
0.15 c/deg
(B)
Firing rate (spikes/s)
Temporal frequency (Hz)
Spatial frequency (c/deg)
(C)
Temporal frequency (Hz)
Spatial frequency (c/deg)

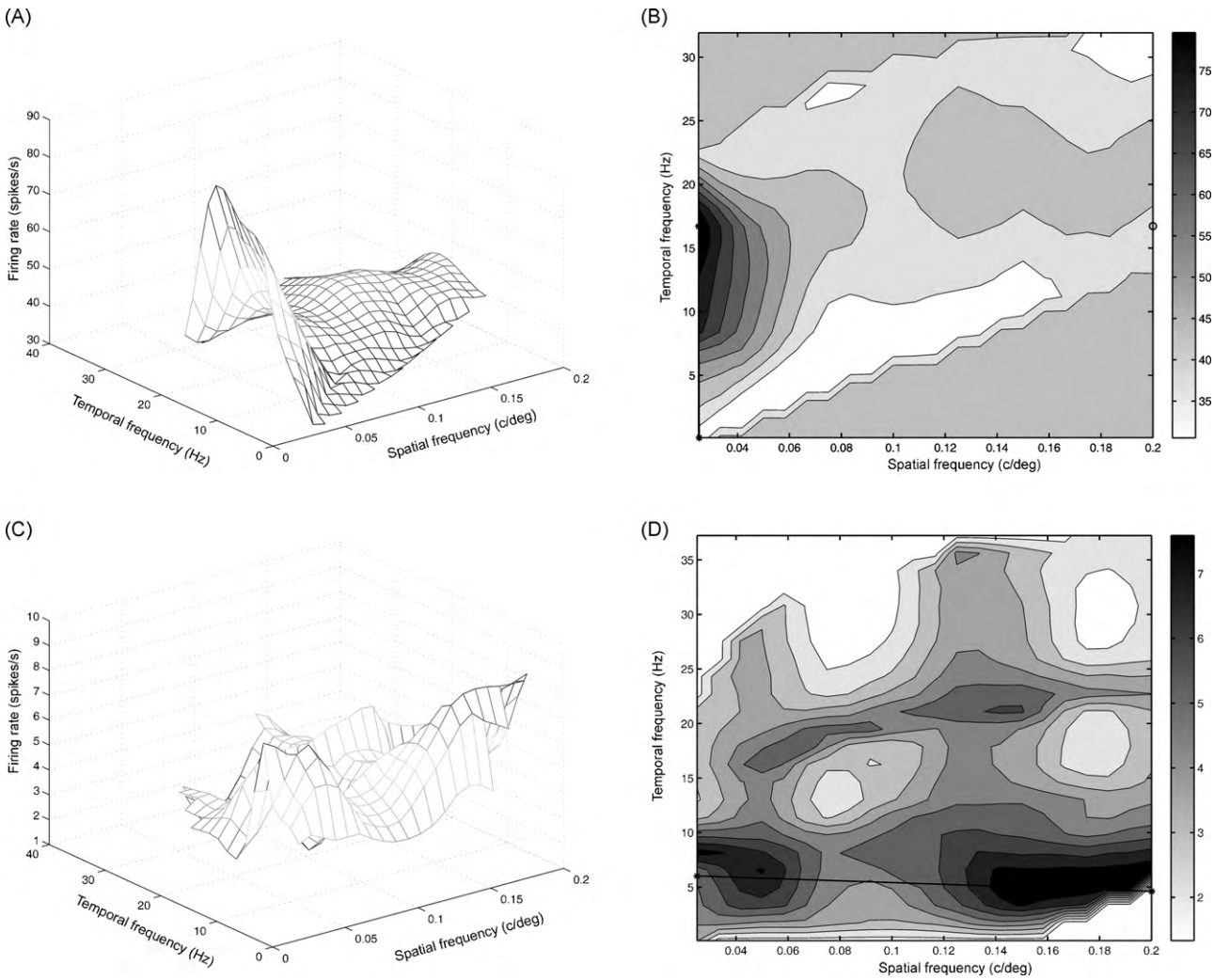


**Fig. 2.** Examples of CN cells with peak and temporal frequency tuned spectral receptive fields. Perspective (A) and contour plots (B), of the spectral RF of a peak tuned CN neuron that responded to the lowest spatial and high temporal frequencies. Perspective (C) and contour plots (D), of the spectral RF of a temporal frequency tuned CN neuron. The conventions are the same as in Fig. 1.

large majority of the peak tuned CN neurons (52/62, 84%) exhibited the same spatial and temporal preferences, responded optimally to the lowest spatial frequencies that we used and also to very high temporal frequencies (Fig. 2A and B). These neurons exhibited low-pass spatial frequency tuning and high-pass or band-pass tuning in the temporal frequency domain. The remaining 10 CN units in this group (10/64, 16%) responded optimally also to low (lower than 0.15 c/°) but not the lowest spatial frequency tested (Fig. 1) and beside the low-pass tuning spatial band-pass tuning was also found. These units responded optimally to high and sometimes moderate temporal frequencies and displayed band-pass temporal frequency tuning. The mean optimum velocity of moving gratings (optimal temporal frequency/optimal spatial frequency) for neurons showing peak tuning was $261 \pm 127$°/s ($N = 62$, range: 40–598°/s).

In a quarter of the recorded population (21/83; 26%), ridge tuned spatio-temporal spectral receptive fields were found. These CN neuron (52/62, 84%), responded optimally also to the low spatial and to moderate and sometimes high temporal frequencies. These neurons showed low-pass and band-pass spatial frequency tuning and band-pass tuning in the temporal frequency domain. In these cases the region of increased activity formed an elongated ridge of peak sensitivity parallel or angled to the temporal or the spatial frequency axis, indicating spatial, temporal or speed tuning, respectively (for classification see Ref. [3]). The mean optimum velocity for these neurons was $159 \pm 76$°/s ($N = 21$, range: 22–444°/s). The velocity preference of the CN neurons with ridge tuning is significantly lower ($p = 0.016$) than that of the CN neurons with peak tuning. Thirteen of the 83 CN units (16%) exhibited temporal fre-

**Fig. 1.** Construction of the spectral receptive fields (RFs). (A) Peristimulus time histograms (PSTHs) depicting the responses of one caudate nucleus (CN) unit to sinusoidal gratings drifting in the preferred direction at various spatial and temporal frequency combinations. The actual spatial frequency values (c/°) are given under each column while the corresponding temporal frequencies (Hz) are given above each PSTH. The thick lines below the histograms indicate the movement of the stimulus for 1 s. The bin width was 20 ms. (B) Perspective mesh plot of the spectral RF of this CN unit. The surface of the mesh was constructed by fitting to the responses, which are shown in part (A) to drifting gratings of different spatial and temporal frequencies. The three axes show the spatial frequency (c/°), the temporal frequency (Hz) of the sinewave grating and the firing rates of a neuron (spikes/s) responding to the particular spatio-temporal frequency combinations, respectively. (C) Contour plot of the spectral RF. The abscissa denotes the spatial frequency of the grating (c/°) while the ordinate denotes the temporal frequency of the grating (Hz). The white points in the contour plot correspond to the neuronal responses demonstrated on PSTHs on part A. The neuronal responses are contour intensity coded; the calibration (spikes/s) can be seen on the right side of the contour plot. The solid line denotes the main direction assigned by principal component analysis (PCA).

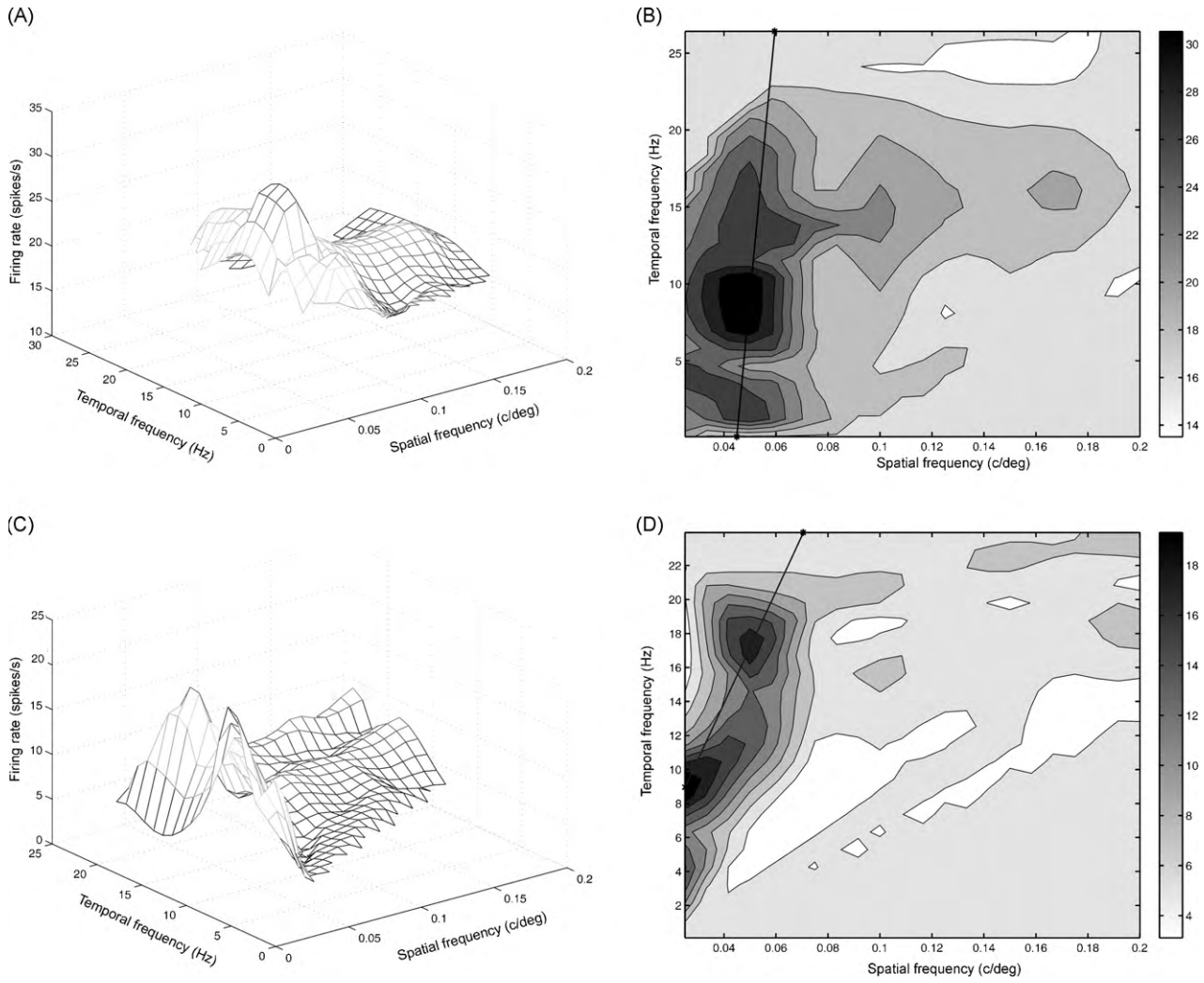


**Fig. 3.** Examples of CN cells with spatial frequency tuned and speed-tuned spectral receptive fields. Perspective (A) and contour plots (B), of the spectral RF of a spatial frequency tuned CN neuron. Perspective (C) and contour plots (D), of the spectral RF of a speed-tuned CN neuron. The conventions are the same as in Fig. 1.

quency tuning, four (5%) spatial frequency tuning and also four (5%) speed tuning. Spectral receptive fields of cells that exhibited temporal frequency tuning (with response domains parallel to the spatial frequency axis) are shown in Fig. 2C and D. In Fig. 3A and B, the spectral RF of a CN cell, which was sensitive to a particular spatial frequency is presented. The response profile of this neuron displays an elongated ridge over a wide range of temporal frequencies in the limited range of spatial frequencies (spatial tuning). Fig. 3C and D shows the spectral RF of a neuron for which the response to spatial frequency varied depending on the temporal frequency of the stimulus, forming a steep domain of peak sensitivity oriented diagonal to the spatial and temporal frequency axes, indicating speed tuning.

In spite of the large number of electrophysiological studies on the CN, little information is available on the visual responsiveness of the CN neurons and hitherto no study addressed the description of spatio-temporal spectral RF organization of striatal neurons. In order to give the first description of the detailed spatio-temporal frequency response profiles of the CN units we tested the responsiveness of these neurons to a wide range of spatial and temporal frequency combinations. We found peak, spatial, temporal and speed-tuned neurons in the CN and we are proposing a new functional classification of the visually active neurons concerning their spectral receptive field organization.

Regarding the spatio-temporal frequency response properties observed in our experiments, we can classify the CN units into the following groups: peak tuned cells, temporally tuned neurons, spatially tuned neurons and speed-tuned neurons [3]. Almost three-quarter of the investigated SC units exhibited peak tuning, characterized by a region of increased activity with a single maximum in the spatio-temporal frequency domain. These neurons responded in a broad range of high velocities with a preference for velocity determined by their optimal spatial and temporal frequencies. The majority of these peak tuned cells in our sample (84%) had RF profiles showing maximum sensitivity at the lowest spatial frequencies and relatively high temporal frequencies. Cells with such spectral RFs in the CN may correspond to SC high velocity excitatory cells [22,23].

The remaining one-quarter of the CN units exhibited ridge tuned spatio-temporal spectral receptive fields. In these cases the regions showing increased activity on the RFs were elongated, forming a ridge of peak sensitivity parallel to the temporal or the spatial frequency axis or oriented relative to the axes indicating spatial, temporal or speed tuning, respectively. The velocity preference of these neurons was significantly lower than that of the peak tuned CN neurons. This may indicate that these neurons do not primarily act as high velocity detectors but rather code motion-related moderate – and rarely lower – velocity changes. The spatio-temporal frequency response characteristics of the three ridge tuned groups of CN neurons indicate that these cells may receive input from and correspond to the low velocity excitatory cells described earlier in

the SC [22,23] distinguished on the basis of their velocity response profiles. The majority of the ridge tuned CN neurons possessed temporal frequency tuning. Here the optimal temporal frequency is invariant with respect to the spatial frequency. Thus these neurons were capable of coding changes in the visual environment with a particular temporal frequency irrespectively from the spatial frequencies that may suggest that the activity of these neurons is independent from the size of the stimulus. A smaller proportion of the ridge tuned CN neurons showed spatial tuning, where the optimal spatial frequency is independent of the temporal frequency. These neurons could code the movement of a stimulus with a particular size, irrespectively of the temporal frequency of the motion. Some CN neurons showed speed tuning, demonstrated spectral RFs forming an elongated ridge of peak sensitivity oriented diagonal to the spatial and temporal frequency axes. This indicates that these neurons responded selectively to a set of particular spatio-temporal frequency combinations, i.e. to a certain speed of stimulus movement.

The spatio-temporal response characteristics found in the CN are in line with the notion that the CN is involved in motion detection and less sensitive to detect static visual events [11,13]. We argue that this visual activity in the CN may be the sensory feedback of motor actions controlled by the basal ganglia and therefore it is necessary for the normal sensory-motor function of the CN. The preference for consistently low spatial frequencies combined with moderate and high temporal frequencies indicates that the visually active CN cells could respond well to large objects moving at a wide range of higher velocities. The peak tuned neurons could encode a certain relatively high velocity, while the ridge tuned neurons are responsible for the detection of moderate and lower velocities. The speed-tuned CN neurons are most probably involved in the detection of objects moving with a particular moderate velocity, while the spatial and temporal tuned CN neurons are most likely involved in detection of stimuli in a broader range of moderate velocities. Thus, we suggest that the wide variety of spatio-temporal frequency response profiles might represents different functional neuronal groups within the CN that subserve different behaviors needed to meet various environmental requirements.

## Acknowledgement

The authors thank Ágnes Farkas, Péter Gombkötõ, Zsuzsanna Paróczy and Zita Márkus for their participation in the data collection; Gabriella Dósai and Joanna Smyda for their technical assistance, and Péter Liszli for the software developement. This work was supported by the grants OTKA/Hungary 75156, OTKA/Hungary 68594, MSHE/Poland N N303 070234 and Bilateral Grant No. 14 supporting joint collaboration from the Polish and Hungarian Academy of Science. A.N. is a János Bolyai Research Fellow of the Hungarian Academy of Science.

## References

[1] P. Barneoud, E. Descombris, N. Aubin, D.N. Abrous, Evaluation of simple and complex sensorimotor behaviours in rats with a partial lesion of the dopaminergic nigrostriatal system, Eur. J. Neurosci. 12 (2000) 322–336.
[2] V.J. Brown, R. Desimone, M. Mishkin, Responses of cells in the tail of the caudate nucleus during visual discrimination learning, J. Neurophysiol. 74 (1995) 1083–1094.
[3] C.W. Clifford, M.R. Ibbotson, Fundamental mechanisms of visual motion detection: models, cells and functions, Prog. Neurobiol. 68 (2003) 409–437.
[4] K.K. De Valois, R.L. De Valois, E.W. Yund, Responses of striate cortex cells to grating and checkerboard patterns, J. Physiol. 291 (1979) 483–505.
[5] J.K. Harting, B.V. Updyke, D.P. Van Lieshout, The visual-oculomotor striatum of the cat: functional relationship to the superior colliculus, Exp. Brain Res. 136 (2001) 138–142.
[6] O. Hikosaka, M. Sakamoto, S. Usui, Functional properties of monkey caudate neurons. II. Visual and auditory responses, J. Neurophysiol. 61 (1989) 799–813.
[7] H. Hollander, J. Tietze, H. Distel, An autoradiographic study of the subcortical projections of the rabbit striate cortex in the adult and during postnatal development, J. Comp. Neurol. 184 (1979) 783–794.
[8] K. Hoshino, G. Eördegh, A. Nagy, G. Benedek, M. Norita, Overlap of nigrothalamic terminals and thalamostriatal neurons in the feline lateralis medialis-suprageniculate nucleus, Acta Physiol. Hung. 96 (2009) 203–211.
[9] E. Lynd-Balta, S.N. Haber, The organization of midbrain projections to the striatum in the primate: sensorimotor-related striatum versus ventral striatum, Neuroscience 59 (1994) 625–640.
[10] Z. Márkus, A. Berényi, Z. Paróczy, M. Wypych, W.J. Waleszczyk, G. Benedek, A. Nagy, Spatial and temporal visual properties of the neurons in the intermediate layers of the superior colliculus, Neurosci. Lett. 454 (2009) 76–80.
[11] A. Nagy, G. Eördegh, M. Norita, G. Benedek, Visual receptive field properties of neurons in the feline caudate nucleus, Eur. J. Neurosci. 18 (2003) 449–452.
[12] A. Nagy, G. Eördegh, G. Benedek, Spatial and temporal visual properties of single neurons in the feline anterior ectosylvian visual area, Exp. Brain Res. 151 (2003) 108–114.
[13] A. Nagy, Z. Paróczy, Z. Márkus, A. Berényi, M. Wypych, W.J. Waleszczyk, G. Benedek, Drifting grating stimulation reveals particular activation properties of visual neurons in the caudate nucleus, Eur. J. Neurosci. 27 (2008) 1801–1808.
[14] M. Norita, J.G. McHaffie, H. Shimizu, B.E. Stein, The corticostriatal and corticotectal projections of the feline lateral suprasylvian cortex demonstrated with anterograde biocytin and retrograde fluorescent techniques, Neurosci. Res. 10 (1991) 149–155.
[15] Z. Paróczy, A. Nagy, Z. Márkus, W.J. Waleszczyk, M. Wypych, G. Benedek, Spatial and temporal visual properties of single neurons in the suprageniculate nucleus of the thalamus, Neuroscience 137 (2006) 1397–1404.
[16] R.B. Pinter, L.R. Harris, Temporal and spatial response characteristics of the cat superior colliculus, Brain Res. 207 (1981) 73–94.
[17] C. Pouderoux, E. Freton, Patterns of unit responses to visual stimuli in the cat caudate nucleus under chloralose anesthesia, Neurosci. Lett. 11 (1979) 53–58.
[18] E.T. Rolls, S.J. Thorpe, S.P. Maddison, Responses of striatal neurons in the behaving monkey. 1. Head of the caudate nucleus, Behav. Brain Res. 7 (1983) 179–210.
[19] J.A. Saint-Cyr, L.G. Ungerleider, R. Desimone, Organization of visual cortical inputs to the striatum and subsequent outputs to the pallido-nigral complex in the monkey, J. Comp. Neurol. 298 (1990) 129–156.
[20] J.M. Schulz, P. Redgrave, C. Mehring, A. Aertsen, K.M. Clements, J.R. Wickens, J.N. Reynolds, Short-latency activation of striatal spiny neurons via subcortical visual pathways, J. Neurosci. 29 (2009) 6336–6347.
[21] E.R. Strecker, G. Steinfels, E.D. Abercrombie, B.L. Jacobs, Caudate unit activity in freely moving cats: effects of phasic auditory and visual stimuli, Brain Res. 329 (1985) 350–353.
[22] W.J. Waleszczyk, C. Wang, W. Burke, B. Dreher, Velocity response profiles of collicular neurons: parallel and convergent visual information channels, Neuroscience 93 (1999) 1063–1076.
[23] W.J. Waleszczyk, A. Nagy, M. Wypych, A. Berényi, Z. Paróczy, G. Eördegh, A. Ghazaryan, G. Benedek, Spectral receptive field properties of neurons in the feline superior colliculus, Exp. Brain Res. 181 (2007) 87–98.